**Supplementary Information for**

**Synaptotagmin-7 deficiency induces mania-like behavioral abnormalities through attenuating GluN2B activity**

Qiu-Wen Wang[a1], Si-Yao Lu[a1], Yao-Nan Liu[a1], Yun Chen[a], Hui Wei[b], Wei Shen[a], Yan-Fen Chen[a], Chong-Lei Fu[a], Ying-Han Wang[a], Anbang Dai[a], Xuan Huan[c], Fred H. Gage[d], Qi Xu[b], and Jun Yao[a]

[*1]These authors contributed equally to this study.

Please address correspondence to: Qi Xu (xuqi@pumc.edu.cn) or Jun Yao (jyao@mail.tsinghua.edu.cn).

**This PDF file includes:**

Extended Materials and Methods
Figure S1 to S3.
Table S1 to S3.

## EXTENDED MATERIALS AND METHODS

**Sample collection, genomic DNA extraction, and Syt7 coding regions sequencing**

Anti-coagulated whole blood with EDTA was obtained between 9am and 11am in the morning through venipuncture of a forearm vein. After plasma separation, the remaining cellular fractions were stored at -80°C and transported by dry ice. Total DNA was extracted using QIAamp DNA Mini Kit (Qiagen, Shanghai, China) according to the manufacturer's instructions. DNA purity was assessed by measuring the A260/A280 ratio using NanoDrop2000c (Thermo Scientific, Shanghai, China) and DNA quality was checked by 0.8% agarose gel electrophoresis for a strong band at high molecular weight (>10 kb). The coding regions of *SYT7* gene were confirmed by NCBI and ensemble databases (NCBI ID: NM_001365809, Ensemble ID: ENST00000539008). Coding sequences of *SYT7* were amplified by PCR and detected by bi-directional Sanger sequencing (Sango Biotech, Shanghai, China). The primers are listed in ***SI Appendix*, Table S2**. DNASTAR Lasergene software (version 7.1) was used to analyze Sanger sequencing data. The chi-square test was applied to analyze the difference of genotypic distributions in BD patients and controls.

**Plasmids**

For the lentiviral experiments, a bicistronic lentiviral vector system, pLox Syn-DsRed-Syn-GFP (pLox), was used by substituting either the DsRed or GFP coding sequence or both with the target cDNA sequence. For the Syt7 experiments, the mouse full-length or HA-tagged Syt7 cDNA sequence was used. For the fluorescence imaging experiments, both DsRed and GFP were excluded to avoid fluorescence overlap. The lentiviral CRISPRi system was described previously (1). The sgRNAs were designed to target the DNA region from -50 to 300 bp relative to the TSS of Syt7 (2).

**Lentivirus preparation and infection**

Lentiviral particles were generated by cotransfecting HEK 293FT cells with virus packaging vectors. HEK 293FT cells were maintained in Dulbecco's modified eagle medium (DMEM) in 10% FBS, 100 units/ml streptomycin and 100 mg/ml penicillin with 2 mM glutamax (Life Technologies). Transfection was performed using PEI (Polysciences). Five hours after transfection, the medium was changed. Virus supernatant was harvested 60 h post-transfection, filtered with a 0.22 μm PVDF filter (Millipore), ultracentrifuged at 25,000 rpm using a P28S rotor (Hitachi) and stocked in a final volume of 100 μl. The titer of the lentivirus used in all cell culture experiments was at least 5.0 X $10^8$ infectious units (IU) per ml.

**Behavioral assays**

Syt7 KO mice were kindly provided by E.R. Chapman (Madison, Wisconsin, USA) with permission from N.W. Andrews (College Park, MD, USA). All the animal experiments were conducted using 3- to 6-month-old male mice under the guidance and approval of the Institutional Animal Care & Use Committee of Tsinghua University and the Animal Welfare and Ethics Committee of Tsinghua University (Approval ID: 15-YJ2). The mice were housed at a constant temperature under a 7:00 to 19:00 12h:12h light/dark cycle (~200 lux white ambient illumination). WT siblings of similar age were used as a

control for the Syt7 KO mice. Different groups of mice were used for dark phase and light phase testing. Activity was recorded by a suspended digital camera and analyzed by EthoVision XT 11.5 (Noldus) after 30 min habituation in the test room (600 lx) in light/dark box test and open field test. The same parameter setting for the definition of each behavior was applied for all the mice tested in different behavior tests. For the drug treatment experiment, unless specified, the drug solutions or vesicle control were injected or infused 30 min before the behavioral tests at the indicated dose. Each group of animals was exposed to multiple behavioral tasks with an interval of at least two weeks so that the animals could recover. The FST and LH experiments were always performed in final, and animals were no longer used following these two paradigms. In experiments with different drug doses, each dose employed a different group of animals. Following behavioral tests, animals infused with virus were dissected to perform immunostaining analysis to verify virus infection, and animals without appropriate virus infection were excluded from analysis. Animals that accidentally died during the study were included in analysis for all completed tests. The data were analyzed by EthoVision XT 11.5 software (Noldus).

**Forced swim test (FST):** Animals were individually introduced to a cylinder (20 cm diameter × 30 cm height) filled with 15 cm of water (23 ± 1°C) and swam for 6 min under normal light. Immobility time was defined as the time when animals remained floating or motionless, keeping balanced in the water. Data acquisition and analyses were carried out by trained individuals blind to the genotype and treatment during the test.

**Sucrose preference test (SPT):** Mice were held on a 12:12 light/dark cycle with food and water and with the temperature at 21 ± 2°C. The test began at the dark phase of animal activity. Mice were placed individually in a chamber equipped with two bottles on opposite walls throughout the experiment (36 h). One bottle was filled with 2% sucrose solution and the other bottle was filled with water. The mice were habituated in the chamber for 12 h. Then the bottles of sucrose solution and water were weighed at 12-, 24-, and 36-h time points to determine the sucrose and water intake in the dark and light phases. To avoid any confounding effect of side preference, the position of the sucrose and water bottles was exchanged every 6 h. Sucrose preferences were calculated as follows: sucrose consumed/(sucrose consumed + water consumed).

**Learned helplessness test (LH):** The learned helplessness model consisted of 3 different phases: inescapable shock training, learned helplessness screening, and the test. Mice were placed in 1 chamber of 2-chamber shuttle boxes (MedAssociates) for a 5-min adaptation period before the test. During the inescapable shock training phase (day 1 to 3), the mice received 120 inescapable foot-shocks (0.45 mA, 15 s duration, randomized average inter-shock interval 45 s) with the door closed between the 2 chambers of the shuttle boxes each day. For the learned helplessness screening phase (day 4), the door was raised at the onset of the shock (0.45 mA) and the shock ended either when the mouse stepped through to the other side of the shuttle boxes or after 3 s. Mice that had more than 5 escape failures developed helplessness behavior during the 10 screening shocks. On the test day, the animals were placed in the shuttle boxes and 0.45-mA shocks were delivered concomitantly with door opening for the first 5 trials, followed by a 2-s delay for the next 40 trials and inter-trial intervals were randomized at an average of 30 s. The shock was terminated either when the animal crossed over to the second chamber or after 24 s. Latency to step through the door and the number of escape failures were

recorded for the last 40 trials by automated software (MED-PC IV).

**Light/dark box (LDB) test:** Mice were placed singly in the dark side of the light/dark box apparatus and allowed to move freely for 10 min; the time spent in the light box was analyzed.

## Electrophysiology

Whole-cell recordings were performed in voltage-clamp mode using a MultiClamp 700B amplifier (Molecular Devices). For acute slice preparation, P30–P50 animals were euthanized under Pentobarbitol Sodium. Brains were removed and placed in ice-cold solution containing (in mM): 110 choline chloride, 25 $NaHCO_3$, 7 $MgCl_2$, 2.5 KCl, 1.3 $NaH_2PO_4$, 0.5 $CaCl_2$, 1.3 Na-asorbate, 0.6 Na-pyruvate and 20 D-glucose. 300-µm-thick slices for hippocampus were prepared on a Compresstome VF-330 vibrotome (Precisionary Instruments). Slices were transferred for 60 min to 33°C artificial cerebrospinal solution (ACSF) containing (in mM): 124 NaCl, 26 $NaHCO_3$, 10 glucose, 3 KCl, 2 $CaCl_2$, 1.25 $KH_2PO_4$ and 1 $MgCl_2$. Whole-cell patch-clamp recordings were performed from hippocampus slice at $33 \pm 1$°C with flow rates of 2 ml/min in ACSF containing 2mM $CaCl_2$. For cultured neuron recording, the recording chamber was continuously perfused with a bath solution (128 mM NaCl, 30 mM glucose, 5 mM KCl, 1 mM $MgCl_2$, 25 mM HEPES; pH 7.3) containing 2 or 0.2 mM $CaCl_2$ via a Warner (Hamden, CT) VC-6 drug delivery system. To isolate NMDAR-EPSCs, 20 µM bicuculline (GABAR antagonist; Sigma), 20 µM CNQX (AMPAR antagonist; Sigma), 10 µM glycine (NMDAR co-agonist; Sigma) and 1 µM Strychnine (glycine receptor antagonist; Sigma) were applied, and $MgCl_2$ was excluded from the extracellular solution. Depending on the experiments, 1 µM Ro25-6981 (Tocris) was used to abolish GluN2B activity, and 50 µM D-AP5 (Tocris) was applied to block all NMDARs. To record evoked EPSCs, presynaptic neurons were depolarized with a theta stimulating electrode with a voltage step from 0 V to 20-30 V for 1 millisecond to trigger an action potential; evoked synaptic release was recorded from the postsynaptic neurons. Patch pipettes were pulled from borosilicate glass and had resistances of 3–5 MΩ when filled with internal pipette solution (130 mM K-gluconate, 1 mM EGTA, 5 mM Na-phosphocreatine, 2 mM Mg-ATP, 0.3 mM Na-GTP, 5 mM QX-314, 10mM HEPES; pH 7.3). The series resistance was typically <15 MΩ and was partially compensated to 60–80%. The membrane potential was held at -70 mV. Data were acquired using pClamp10 software (Molecular Devices), sampled at 10 kHz, and filtered at 2 kHz. Off-line data analysis of EPSCs was performed using Clampfit software (Molecular Devices).

## STORM imaging

For cultured cell imaging, hippocampal neurons were fixed with 4% paraformaldehyde (PFA) and 0.1% glutaradehyde in phosphate-buffered saline (PBS; pH 7.4) for 10 min, followed by washing off excess PFA and reducing unreacted aldehyde groups with 0.1% sodium borohydride ($NaBH_4$) in PBS. Cells were then blocked and permeabilized in blocking buffer (3% w/v BSA, 0.2% v/v Triton X-100 in PBS) for 1 h at room temperature, followed by incubation with primary and secondary antibodies, each for 2 h at room temperature. After washing, cells were post-fixed for 10 min with 4% PFA and 0.1% glutaraldehyde in PBS and used for STORM imaging. For slice imaging experiments, mice were anesthetized and dissected. Followed by 4% PFA fixation and

30% sucrose dehydration, brains were freshly frozen by embedding into Tissue-tek OCT medium. Sections of 10 μm thickness were cut on a cryostat and collected on PBS. Sections were fixed for 15 min with 4% PFA and 0.2% glutaraldehyde, followed by washing off excess PFA and quenching used the 0.1% NaBH$_4$. Sections were then blocked and permeabilized, followed by incubation with primary antibody overnight at 4°C and secondary antibodies for 2 hr at room temperature, and finally post-fixed for 5 min in 3% PFA and 0.05% glutaraldehyde in PBS. Primary antibodies include rabbit polyclonal anti-vGLUT1 antibody (1:300, Abcam, #ab104898), rabbit polyclonal anti-Syt7 antibody (1:200, Synaptic Systems, #105173), rabbit polyclonal anti-phospho-GluN2A antibody (1:200, Abcam, #ab16646), rabbit polyclonal anti-GluN2B antibody (1:200, Abcam, #ab65783), mouse monoclonal anti-PSD95 antibody (1:300, Millipore, #MAB1598), and Guinea pig polyclonal anti-vGLUT1 antibody (1:200, Synaptic Systems, #135304). Secondary antibodies include donkey anti-rabbit AleaxFlour568 antibody (1:500, Life Technologies, #a10042), goat anti-mouse ATTO488 antibody (1:500, Lockland, #610-152-121S), goat anti-Guinea pig AleaxFlour568 antibody (1:500, Life Technologies, #a11075), goat anti-rabbit AleaxFlour647 antibody (1:500, Life Technologies, #a21245), and donkey anti-chicken AleaxFlour647 antibody (1:500, Jackson Immunoresearch, #703605155).

Imaging experiments were performed using a Nikon combined Confocal A1/SIM/STORM system with 4 activation/imaging lasers (405 nm, 488nm and 561nm from Coherent, 647nm from MPBC) and a CFI Apo SR TIRF 100X oil (NA 1.49) objective. The images were acquired with an Andor EMCCD camera iXON 897. STORM imaging was performed in imaging buffer containing 50 mM Tris (pH 8.0) and 10 mM NaCl, a previously described oxygen scavenging system (3) (1.2 mg/ml glucose oxidase (Sigma-Aldrich), 73 μm/ml catalase (Sigma-Aldrich) and 10% (w/v) glucose) and 304 mM β-mercaptoethylamine (Sigma-Aldrich). Prior to STORM imaging, confocal images for different color channels were acquired to identify the region of interest. Three-dimensional multi-channel STORM data acquisition was then performed. We used sequential collection mode from 647 nm to 488 nm as follows: 1) Alexa647 signal was collected first while the other 2 dyes were not excited; 2) when Alexa647 was bleached mostly, the 561 nm laser was turned on to collect the Alexa568 signal; 3) the Atto488 signal was collected last. For Atto488 and Alexa568, we used the 405 nm laser as the activation laser to guarantee the efficiency of the data acquisition. Data analysis was performed using NIS-Elements AR (Nikon) software. Following 3-D reconstruction, lateral and axial drift in the sample during acquisition was corrected as described previously (4). Puncta with juxtaposed vGLUT1 and PSD95 signals were selected as a synapse for analysis. The image was rotated so that the trans-synaptic axis and the long and short axes could be aligned along the x, y, and z axes, respectively.

**SIM imaging**

Hippocampal neurons were cultured in a 10-mm confocal dish. Cells were washed with PBS 3 times and put in a bath solution consisting of 140 mM NaCl, 5 mM KCl, 2 mM MgCl$_2$, 10 mM HEPES, 10 mM glucose, 10 μM CNQX, and 50 μM d-AP5 (pH 7.4). CaCl$_2$ or SrCl$_2$ at different concentrations was added to the bath solution according to the requirements of the experiments. Two-dimensional SIM imaging was performed using a Nikon combined Confocal A1/SIM/STORM system equipped with a CFI Apo SR TIRF

100X oil (NA 1.49) objective, 488 nm laser and the corresponding dichroic and filter sets, and an Andor EMCCD camera iXON 897. Images were acquired at a frequency of 0.4 Hz. During the imaging process, a 10-s 20 Hz field train stimulation was elicited at 30 s using a SD-9 stimulator (Grass Technologies). Puncta showing fluorescence changes in response to stimulation were selected as regions of interest (ROI). Reconstruction of the 2D-SIM images was carried out with NIS-Elements AR software (Nikon Instruments). The fluorescence intensity of each pixel was projected onto the x-axis, and the full width at half maxima (FWHM) with Gaussian fitting along the x-axis was analyzed using MATLAB software (MathWorks). For the dynamics analysis, the fluorescence of the image right before stimulation was employed as the baseline. The fluorescence change from the baseline was used as $\Delta F$, the maximal fluorescence during the imaging process was used as F, and the value of $\Delta F/F$ was used for dynamics comparison.

**Differentiation of iPSCs into DG-like neurons**

The forebrain neural progenitor cells (NPCs) derived from BD patients and healthy people were characterized as previously described (5). The information about the approving committee, informed consent and clinical trial registration number of the iPSC studies was described in the original articles (5). To obtain hippocampal DG-like neurons, NPCs were differentiated in DMEM/F12 supplemented with N2 (Life Technologies), B27 (Life Technologies), 20 ng/ml BDNF (Peprotech), 1 mM dibutyrl-cyclicAMP (Sigma), 200 nM ascorbic acid (Sigma), 1 µg/ml Laminin, and 620 ng/ml Wnt3a (R&D) for 3 to 4 weeks. Wnt3a was removed after 3 weeks. Neurons differentiated for 3-6 weeks were used for imaging and electrophysiological analyses. All cells used in the present study were verified as mycoplasma contamination free.

**Immunoblot analysis**

Neurons were lysed in RIPA buffer (50 mM Tris-Cl, pH 8.0, 150 mM NaCl, 1% Nonidet P-40, 0.5% sodium deoxycholate and 0.1% SDS) plus a complete protease inhibitor cocktail (Roche). Lysates were centrifuged and supernatants were subjected to SDS-PAGE. The blots were developed using an ECL kit (Pierce). Protein levels were quantified by densitometry using NIH ImageJ 1.48 software. Primary antibodies were as follows: rabbit polyclonal anti-phospho-GluN2A antibody (1:500, Abcam, #ab16646), rabbit polyclonal anti-GluN2B antibody (1:500, Abcam, #65783), mouse anti-β-tubulin monoclonal antibody (1:2000, Sigma, T5076), rabbit polyclonal anti-Syt7 antibody (1:500, Synaptic Systems, #105173), chicken polyclonal anti-HA antibody (1:1000, Abcam, #ab9111), and mouse monoclonal anti-Actin antibody (1:5000, Abcam, #ab6276).

**Immunofluorescence**

Mice were euthanized 2 weeks after viral delivery and transcardially perfused with 4% PFA in PBS. Fixed tissue was sectioned with 50-µm thickness using vibratome (Leica, VT1000S). Then antigens were retrieved by incubating for 10 min in 100 mM Tris (pH 7.4). Sections were blocked with 5% normal goat serum (NGS) in TBST (137 mM NaCl, 20 mM Tris pH 7.6, 0.05% Tween-20) for 1 h and incubated with primary antibodies overnight at 4°C. After 3 washes in TBST, samples were incubated with secondary antibodies. Following 3 washes with TBS, cells were incubated with DAPI (0.1 µg/ml, Sigma) for 15 min, followed by 3 washes with TBS to remove DAPI. Fluorescent signals

were detected on an Olympus FV1200 confocal microscope by sequential acquisition or on slide scanner (Zeiss, Axio Scan.Z1) and images were processed using ImageJ 1.48 software (NIH). Primary antibodies were as follows: rabbit polyclonal anti-Prox1 antibody (1:500, Abcam, #ab101851), and mouse monoclonal anti-Tuj1 antibody (1:500, Sigma, #T5076). Secondary antibodies were as follows: goat anti-mouse AleaxFlour488 antibody (1:500, JacksonImmuno, #115-546-003), and goat anti-rabbit AleaxFlour647 antibody (1:500, JacksonImmuno, #111-606-003).

**Reverse transcription PCR**

Total RNA was isolated using Trizol (Life Technologies) according to the manufacturer's instructions. cDNA was synthesized using SuperScript III Reverse Transcription Kit (Life Technologies). The primer sequences for PCR are listed in *SI Appendix*, **Table S2**. Quantitative reverse transcription PCR (qRT-PCR) was performed on a Bio-Rad CFX96 thermal cycler using SYBR green supermix (Bio-Rad) and gene-specific primers. Quantitative analysis was performed employing the $\Delta\Delta CT$ method and the GAPDH as the endogenous control.

**Statistical analysis**

Data are shown as mean values ± SEM. Two-way ANOVA analysis for experiments in **Fig. 1*A* and 1*B*** was listed in **Fig. 1 and Fig. 2**; two-tailed unpaired Student's *t*-test was used for all other experiments and was listed in figures; Two-way ANOVA analysis for experiments other than **Fig. 1*A*** and **1*B*** was listed in *SI Appendix,* **Fig. S3**. Multiple comparisons between the groups were performed using the S-N-K method. In the figures, quantification is represented as a box-and-whisker plot with upper and lower whiskers representing the maximum and minimum values, respectively; the boxes represent 2.5%, median and 97.5% quartiles. The analysis approaches have been justified as appropriate by previous biological studies, and all data met the criteria of normal distribution. The statistical data for all experiments are listed in *SI Appendix*, **Table S3**. Statistical significance was evaluated at p<0.05.

*REFERENCES*

1.  Zheng Y*, et al.* (2018) CRISPR interference-based specific and efficient gene inactivation in the brain. *Nature neuroscience*.
2.  Gilbert LA*, et al.* (2014) Genome-scale CRISPR-mediated control of gene repression and activation. *Cell* 159(3):647-661.
3.  Ha T*, et al.* (2002) Initiation and re-initiation of DNA unwinding by the Escherichia coli Rep helicase. *Nature* 419(6907):638-641.
4.  Huang B, Wang W, Bates M, & Zhuang X (2008) Three-dimensional super-resolution imaging by stochastic optical reconstruction microscopy. *Science* 319(5864):810-813.
5.  Mertens J*, et al.* (2015) Differential responses to lithium in hyperexcitable neurons from patients with bipolar disorder. *Nature* 527(7576):95-99.
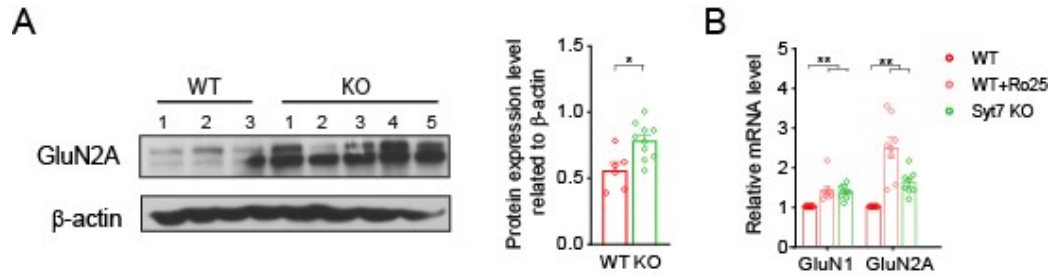
**Fig. S1. Expression of NMDAR subunits in the hippocampus of Syt7 KO mice.** (**A**) Immunoblot showing an enhanced expression of GluN2A in the hippocampus of Syt7 KO mice. WT: n = 36; KO: n = 10. (**B**) qRT-PCR analysis showing increased expression of GluN2A and GluN1 in cultured WT hippocampal neurons treated with Ro25 and Syt7 KO neurons. n = 9. Student's *t*-test; *$P < 0.05$; **$P < 0.001$; error bars, s.e.m.
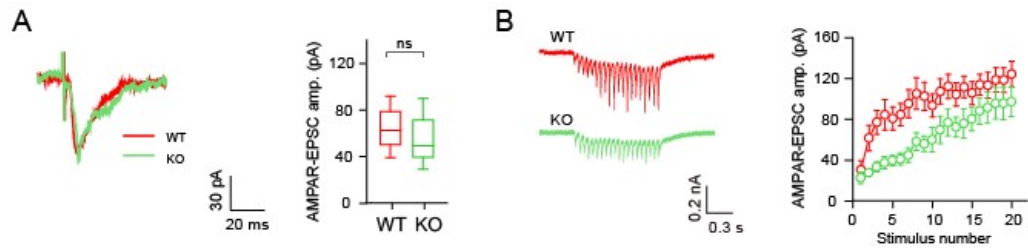
**Fig. S2. Evoked AMPAR-EPSCs in hippocampal slices of Syt7 KO mice.** (**A**) Sample trace (left) and mean amplitude (right) of 2 mM $[Ca^{2+}]$ evoked AMPAR-EPSCs in hippocampal slices of WT and Syt7 KO mice. n = 20 neurons of 3 mice. (**B**) Sample traces (left) and amplitude depression (right) of 2 mM $[Ca^{2+}]$ evoked AMPAR-EPSCs in hippocampal slices. WT. n = 18 neurons of 3 mice; KO, n = 12 neurons of 3 mice. Student's *t*-test; *$P < 0.05$; **$P < 0.001$; error bars, s.e.m.
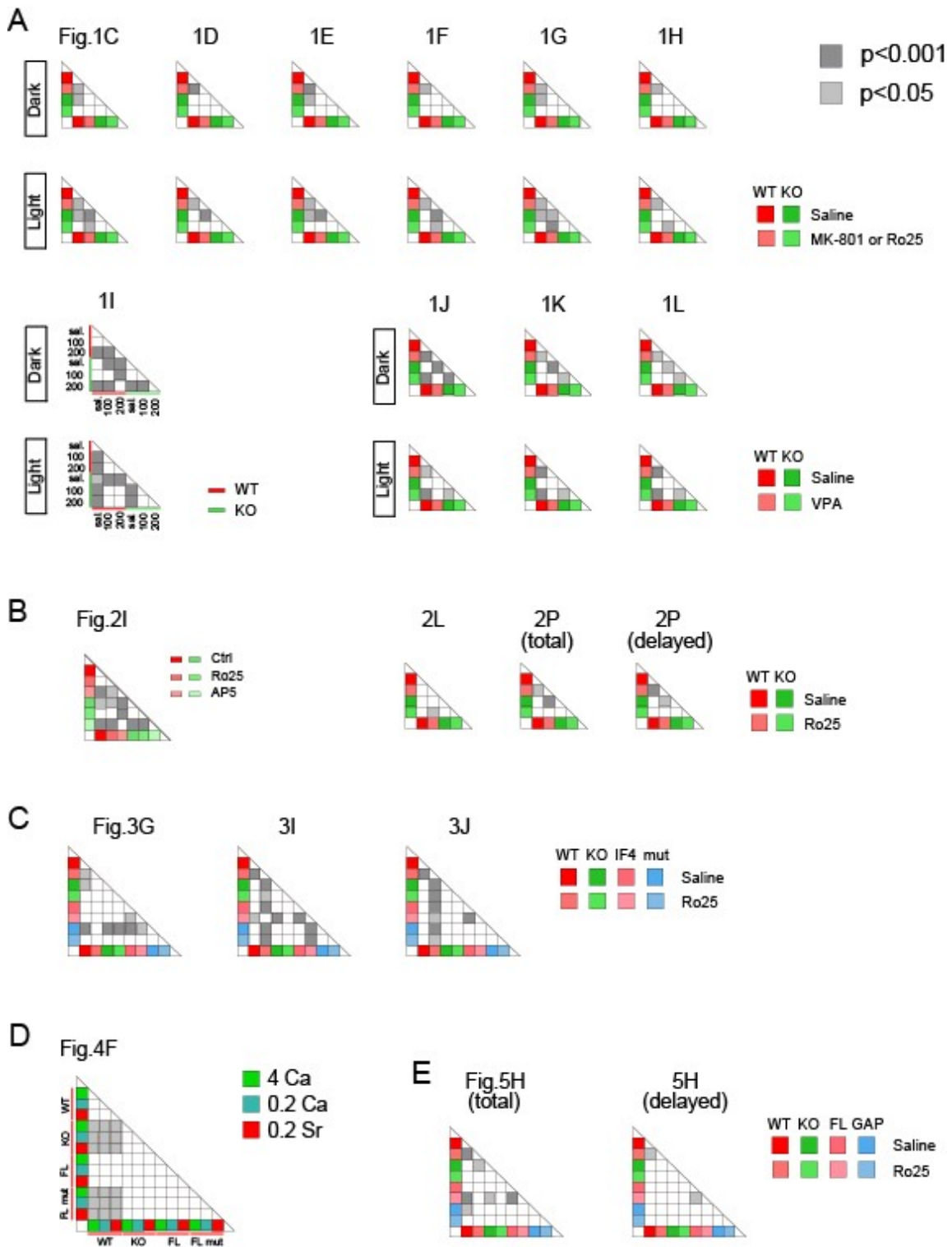
**Fig. S3. Two-way ANOVA analysis of experimental results.** (**A**) AVOVA test of **Fig. 1C-1L**. (**B**) AVOVA test of **Fig. 2I, 2L and 2P**. (**C**) AVOVA test of **Fig. 3G, 3I and 3J**. (**D**) AVOVA test of **Fig. 4F**. (**E**) AVOVA test of **Fig. 5H**.

**Table S1. Allele frequency distributions of mutations (polymorphisms) in exon 6 of Syt7 gene in BD patients and normal controls**

| Sample ID | Position (GRCh38.p12) | SNP | m/M[a] | Amino Acid Substitution | case MAF[b] | control MAF[b] | $X^2$, df | OR[c] | 95% CI | p[d] |
|---|---|---|---|---|---|---|---|---|---|---|
| 02478 | 61542212 | - | T/G | L314M | 6.87E-04 | 0 | 0.8259, 1 | 2.479 | 0.1008 to 60.95 | 0.3635 |
| 02478 | 61542216 | rs1234738801 | T/G | S312S | 6.87E-04 | 0 | 0.8259, 1 | 2.479 | 0.1008 to 60.95 | 0.3635 |
| 02642 | 61542286 | rs1173094215 | T/C | S289N | | | | | | |
| 02547 | 61542286 | rs1173094215 | T/C | S289N | 0.0014 | 0 | 1.652, 1 | 4.134 | 0.1981 to 86.25 | 0.1986 |
| 02830 | 61542411 | rs1181562465 | A/C | Q247H | | | | | | |
| 02749 | 61542411 | rs1181562465 | A/C | Q247H | 0.0014 | 0 | 1.652, 1 | 4.134 | 0.1981 to 86.25 | 0.1986 |
| 02656 | 61542743 | - | T/G | L227M | 6.87E-04 | 0 | 0.8259, 1 | 2.479 | 0.1008 to 60.95 | 0.3635 |
| Combined | | | | | 0.0041 | 0 | 4.965, 1 | 10.78 | 0.6061 to 191.6 | 0.0259 |

[a] m/M, indicates minor allele/major allele.
[b] MAF: minor allele frequency.
[c] Odds Ratio was calculated by adding 0.5 to each value.
[d] p values were calculated by chi-squared test.

**Table S2. Sequence of primers for PCR analysis.**

2.1 Primers used for qRT-PCR analysis

| Gene | Sequence (5' to 3') |
|---|---|
| *SYT7 (human)* | Forward: 5'-AAGCGGGTGGAGAAGAAGAA-3' |
| | Reverse: 5'-CGAAGGCGAAGGACTCATTG-3' |
| *Syt7 (mouse)* | Forward: 5'-GCTGCTCTTGTCCCTCTGCTAC-3' |
| | Reverse: 5'-CATGGCTTTGAGGTTTCGAGCTTT-3' |
| *GluN2B (mouse)* | Forward: 5'-TAATGGCAGATAAGGATGA-3' |
| | Reverse: 5'-GACGATGGAGAAGATGTA-3' |
| *GluN2A (mouse)* | Forward: 5'-AGGTCAACAGCATCATAT-3' |
| | Reverse: 5'-CAGCATAAGGCATAACAT-3' |
| *GluN1 (mouse)* | Forward: 5'-TGACAATCCACCAAGAAC-3' |
| | Reverse: 5'-ACCATTGACTGTGAACTC-3' |
| *GAPDH (mouse)* | Forward: 5'-ATGACTCCACTCACGGCAAA-3' |
| | Reverse: 5'-TAGACTCCACGACATACTCAGC-3' |
| *SYT7- isform α /4 (mouse)* | Forward: 5'-CAGACGCCACACGATGAGTC-3' |
| | Reverse: 5'-CTGGTAAGGGAGTTGACGAGG-3' |
| *SYT7-isform4 (mouse)* | Forward: 5'-GCCATCAACGACCTAGACAGA-3' |
| | Reverse: 5'-GGCGTAGGGTGAAATGTTTAGA-3' |

2.2 PCR primers for identification of human *SYT7* gene mutations

| Region | Length | Forward sequence | Reverse sequence |
|---|---|---|---|
| Exon1 | 319bp | TCTGAGGAGCCCGGAGG | GAGAGGTCCTTGTGGGGACA |
| Exon2 | 314bp | TTCAGAGCTCCCAGTGAAGG | CCCAAGCCTGTAATTGTGTG |
| Exon3 | 230bp | TAGGGAGGGTACAGTCCT | GTGTGTGGTCAGGTCTGTG |
| Exon4 | 240bp | CAGGACTTGCAGTTCTTGTT | GATACTCGGTACATATGATC |
| Exon5 | 464bp | GTTAACCCATTTGCAGTGCTG | CTGAAATGCATCACTGTATG |
| Exon6 | 533bp | CTCGGCTTCTTTCTCTTCCACT | TACACACAACCAGCTGCTCC |
| Exon7 | 506bp | GGAGTCTCAGGCCGTAGTCAACT | CACCACCACCTCGTCCAGCAG |
| Exon8 | 313bp | GTCTTCAGAGAAGGTCCTG | ATCATTCCCACACACATCCCTC |
| Exon9 | 465bp | TGGGATGTGAGTGTGGGCTG | CACAAGTGTGGTTGGGTAG |
| Exon10 | 597bp | ACTGAGATGGACACAAGGTG | CTTCCTAAGGTTGACAAGGGT |
| Exon11 | 241bp | GCTAGGCCAATCAGAGAGCTCT | TGTAAACCTTGTGTCACCAG |
| Exon12 | 350bp | CTGCCTCAGCTTCCATTCCT | TAAGGAACGGAGCCTCACTG |
| Exon13 | 280bp | ACAGGCTAGGGTATCATGGTG | CGTTGTGCATAAAGTGGTGAG |

**Table S3. Statistical data for all experiments.**

| | | | Fig. 1 |
|---|---|---|---|
| Fig.1A | Dark | WT | Saline: 120.13 ± 13.73 s, n = 8 |
| | | | 0.08 mg/kg B.W.: 89.43 ± 13.50 s, n = 8; p>0.13, compared to saline |
| | | | 0.12 mg/kg B.W.: 46.88 ± 12.17 s, n = 8; p<0.002, compared to saline |
| | | | 0.16 mg/kg B.W.: 35.00 ± 8.05 s, n = 8; p<0.001, compared to saline |
| | | | 0.20 mg/kg B.W.: 26.13 ± 5.35 s, n = 8; p<0.001, compared to saline |
| | | KO | Saline: 68.38 ± 13.23 s, n = 8; p<0.02, compared to WT saline |
| | | | 0.08 mg/kg B.W.: 63.43 ± 7.08 s, n = 8; p>0.75, compared to KO saline; p>0.11, compared to WT 0.08 mg/kg |
| | | | 0.12 mg/kg B.W.: 52.00 ± 11.34 s, n = 8; p>0.36, compared to KO saline; p>0.76, compared to WT 0.12 mg/kg |
| | | | 0.16 mg/kg B.W.: 54.50 ± 8.33 s, n = 8; p>0.35, compared to KO saline; p>0.11, compared to WT 0.16 mg/kg |
| | | | 0.20 mg/kg B.W.: 48.00 ± 6.91 s, n = 8; p>0.19, compared to KO saline; p<0.02, compared to WT 0.20 mg/kg |
| | Light | WT | Saline: 130.78 ± 12.04 s, n = 8 |
| | | | 0.08 mg/kg B.W.: 111.75 ± 17.83 s, n = 8; p>0.38, compared to saline |
| | | | 0.12 mg/kg B.W.: 67.13 ± 8.28 s, n = 8; p<0.001, compared to saline |
| | | | 0.16 mg/kg B.W.: 51.75 ± 10.24 s, n = 8; p<0.001, compared to saline |
| | | | 0.20 mg/kg B.W.: 49.63 ± 5.26 s, n = 8; p<0.001, compared to saline |
| | | KO | Saline: 166.00 ± 11.31 s, n = 8; p<0.05, compared to WT saline |
| | | | 0.08 mg/kg B.W.: 158.00 ± 13.44 s, n = 8; p>0.65, compared to KO saline; p>0.05, compared to WT 0.08 mg/kg |
| | | | 0.12 mg/kg B.W.: 139.50 ± 12.76 s, n = 8; p>0.10, compared to KO saline; p<0.001, compared to WT 0.12 mg/kg |
| | | | 0.16 mg/kg B.W.: 134.75 ± 4.74 s, n = 8; p<0.04, compared to KO saline; p<0.001, compared to WT 0.16 mg/kg |
| | | | 0.20 mg/kg B.W.: 126.00 ± 9.63 s, n = 8; p<0.02, compared to KO saline; p<0.001, compared to WT 0.20 mg/kg |
| Fig.1B | Dark | WT | Saline: 120.13 ± 13.73 s, n = 8 |
| | | | 2.5 mg/kg B.W.: 83.88 ± 10.72 s, n = 8; p<0.05, compared to saline |
| | | | 5.0 mg/kg B.W.: 76.63 ± 6.91 s, n = 8; p<0.02, compared to saline |
| | | | 10 mg/kg B.W.: 52.13 ± 10.92 s, n = 8; p<0.001, compared to saline |
| | | | 15 mg/kg B.W.: 32.00 ± 4.19 s, n = 8; p<0.001, compared to saline |
| | | KO | Saline: 68.38 ± 13.23 s, n = 8; p<0.03, compared to WT saline |
| | | | 2.5 mg/kg B.W.: 55.50 ± 9.14 s, n = 8; p>0.24, compared to KO saline; p>0.06, compared to WT 2.5 mg/kg |
| | | | 5 mg/kg B.W.: 51.13 ± 8.52 s, n = 8; p>0.14, compared to KO saline; p<0.03, compared to WT 5 mg/kg |
| | | | 10 mg/kg B.W.: 54.50 ± 7.63 s, n = 8; p>0.20, compared to KO saline; p>0.86, compared to WT 10 mg/kg |

| | | | |
|---|---|---|---|
| | | | 15 mg/kg B.W.: 50.63 ± 8.59 s, n = 8; p>0.12, compared to KO saline; p<0.05, compared to WT 15 mg/kg |
| | Light | WT | Saline: 127.60 ± 10.51 s, n = 8 |
| | | | 2.5 mg/kg B.W.: 99.88 ± 9.57 s, n = 8; p>0.08, compared to saline |
| | | | 5.0 mg/kg B.W.: 58.38 ± 5.90 s, n = 8; p<0.001, compared to saline |
| | | | 10 mg/kg B.W.: 52.75 ± 6.98 s, n = 8; p<0.001, compared to saline |
| | | | 15 mg/kg B.W.: 43.50 ± 5.66 s, n = 8; p<0.001, compared to saline |
| | | KO | Saline: 164.40 ± 9.33 s, n = 8; p<0.02, compared to WT saline |
| | | | 2.5 mg/kg B.W.: 155.63 ± 16.90 s, n = 8; p>0.61, compared to KO saline; p<0.02, compared to WT 2.5 mg/kg |
| | | | 5 mg/kg B.W.: 145.25 ± 12.93 s, n = 8; p>0.58, compared to KO saline; p<0.001, compared to WT 5 mg/kg |
| | | | 10 mg/kg B.W.: 134.00 ± 16.88 s, n = 8; p>0.06, compared to KO saline; p<0.001, compared to WT 10 mg/kg |
| | | | 15 mg/kg B.W.: 129.50 ± 13.80 s, n = 8; p<0.04, compared to KO saline; p<0.001, compared to WT 15 mg/kg |
| Fig. 1C | Dark | WT | Saline: 31.3 ± 6.5%, n = 8 |
| | | | MK801: 6.9 ± 3.3%, n = 8; p<0.01 |
| | | KO | Saline: 19.5 ± 5.2%, n = 9 |
| | | | MK801: 15.3 ± 7.8%, n = 9; p>0.6 |
| | Light | WT | Saline: 34.7 ± 6.8%, n = 8 |
| | | | MK801: 4.4 ± 2.9%, n = 8; p<0.01 |
| | | KO | Saline: 56.4 ± 6.7%, n = 9 |
| | | | MK801: 40.0 ± 11.4%, n = 9; p>0.2 |
| Fig. 1D | Dark | WT | Saline: 32.8 ± 5.0%, n = 8 |
| | | | RO25: 2.5 ± 1.4%, n = 8; p<0.01 |
| | | KO | Saline: 17.5 ± 5.6%, n = 9 |
| | | | RO25: 18.3 ± 7.6%, n = 9; p>0.5 |
| | Light | WT | Saline: 37.2 ± 8.0%, n = 8 |
| | | | RO25: 5.6 ± 3.7%, n = 8; p<0.01 |
| | | KO | Saline: 57.2 ± 7.0%, n = 9 |
| | | | RO25: 34.7 ± 11.7%, n = 9; p>0.1 |
| Fig. 1E | Dark | WT | Saline: 82.7 ± 1.9%, n = 10 |
| | | | MK801: 94.2 ± 1.7%, n = 10; p<0.001 |
| | | KO | Saline: 90.0 ± 2.3%, n = 10 |
| | | | MK801: 88.1 ± 2.1%, n = 10; p>0.5 |
| | Light | WT | Saline: 80.8 ± 2.4%, n = 10 |
| | | | MK801: 91.6 ± 3.2%, n = 10; p<0.02 |
| | | KO | Saline: 69.5 ± 4.6%, n = 10 |
| | | | MK801: 77.7 ± 4.2%, n = 10; p>0.2 |
| Fig. 1F | Dark | WT | Saline: 80.3 ± 2.8%, n = 10 |
| | | | RO25: 91.6 ± 3.2%, n = 10; p<0.02 |
| | | KO | Saline: 89.2 ± 2.3%, n = 10 |
| | | | RO25: 84.5 ± 2.7%, n = 10; p>0.1 |
| | Light | WT | Saline: 81.1 ± 3.1%, n = 10 |
| | | | RO25: 91.0 ± 3.2%, n = 10; p<0.04 |

| | | | |
|---|---|---|---|
| | | KO | Saline: 79.1 ± 3.7%, n = 10 |
| | | | RO25: 75.2 ± 3.3%, n = 10; p>0.8 |
| Fig. 1G | Dark | WT | Saline: 248.1 ± 15.0, n = 11 |
| | | | MK801: 343.4 ± 30.2, n = 11; p<0.02 |
| | | KO | Saline: 290.7 ± 14.8, n = 11 |
| | | | MK801: 291.8 ± 36.2, n = 11; p>0.9 |
| | Light | WT | Saline: 292.6 ± 12.9, n = 11 |
| | | | MK801: 357.8 ± 23.7, n = 11; p<0.03 |
| | | KO | Saline: 236.5 ± 29.7, n = 11 |
| | | | MK801: 230.7 ± 33.1, n = 11; p>0.8 |
| Fig. 1H | Dark | WT | Saline: 248.1 ± 15.0, n = 11 |
| | | | RO25: 321.7 ± 14.9, n = 11; p<0.01 |
| | | KO | Saline: 290.7 ± 14.8, n = 11 |
| | | | RO25: 286.3 ± 35.3, n = 11; p>0.9 |
| | Light | WT | Saline: 292.6 ± 12.9, n = 11 |
| | | | RO25: 337.6 ± 23.1, n = 11; p<0.05 |
| | | KO | Saline: 236.5 ± 29.7, n = 11 |
| | | | RO25: 234.2 ± 38.5, n = 11; p>0.9 |
| Fig. 1I | Dark | WT | Saline: 123.63 ± 3.04 s, n = 8 |
| | | | 100 mg/kg B.W.: 164.50 ± 12.82 s, n = 8, p<0.001 |
| | | | 200 mg/kg B.W.: 268.63 ± 10.48 s, n = 8, p<0.001 |
| | | KO | Saline: 82.00 ± 15.25 s, n = 8, |
| | | | 100 mg/kg B.W.: 120.50 ± 10.53 s, n = 8; p<0.04, compared to KO saline; p<0.02, compared to WT 100 mg/kg |
| | | | 200 mg/kg B.W.: 268.13 ± 9.05 s, n = 8; p<0.001, compared to KO saline; p>0.97, compared to WT 200 mg/kg |
| | Light | WT | Saline: 135.88 ± 6.28 s, n = 8 |
| | | | 100 mg/kg B.W.: 267.50 ± 11.72 s, n = 8; p<0.001 |
| | | | 200 mg/kg B.W.: 294.25 ± 11.10 s, n = 8; p<0.001 |
| | | KO | Saline: 174.63 ± 6.52 s, n = 8; p<0.001, compared to WT saline |
| | | | 100 mg/kg B.W.: 260.25 ± 7.08 s, n = 8; p<0.001 |
| | | | 200 mg/kg B.W.: 283.25 ± 7.54 s, n = 8; p<0.001 |
| Fig.1J | Dark | WT | Saline: 31.3 ± 4.3%, n = 8 |
| | | | VPA: 75.9 ± 10.9%, n = 8; p<0.01 |
| | | KO | Saline: 20.3 ± 4.4%, n = 9 |
| | | | VPA: 75.9 ± 9.8%, n = 9; p<0.01 |
| | Light | WT | Saline: 37.5 ± 4.9%, n = 8 |
| | | | VPA: 55.3 ± 5.8%, n = 8; p<0.04 |
| | | KO | Saline: 51.7 ± 7.2%, n = 9 |
| | | | VPA: 77.5 ± 5.9%, n = 9; p<0.02 |
| Fig.1K | Dark | WT | Saline: 81.3 ± 3.9%, n = 11 |
| | | | VPA: 66.5 ± 3.5%, n = 11; p<0.01 |
| | | KO | Saline: 90.3 ± 2.4%, n = 11 |
| | | | VPA: 72.8 ± 3.9%, n = 11; p<0.01 |
| | Light | WT | Saline: 81.4 ± 3.0%, n = 11 |
| | | | VPA: 59.9 ± 3.0%, n = 11; p<0.001 |
| | | KO | Saline: 71.3 ± 4.4%, n = 11 |
| | | | VPA: 58.8 ± 3.5%, n = 11; p<0.04 |

| Fig.1L | Dark | WT | Saline: 248.1 ± 15.0, n = 11 |
|---|---|---|---|
| | | | VPA: 211.3 ± 13.2, n = 11; p<0.04 |
| | | KO | Saline: 290.7 ± 14.8, n = 11 |
| | | | VPA: 215.2 ± 23.5, n = 11; p<0.02 |
| | Light | WT | Saline: 292.6 ± 12.9, n = 11 |
| | | | VPA: 139.4 ± 33.3, n = 11; p<0.001 |
| | | KO | Saline: 236.5 ± 29.7, n = 11 |
| | | | VPA: 115.0 ± 29.1, n = 11; p<0.01 |
| | | | |
| | | | Fig. 2 |
| Fig. 2G | WT | | 1.31 ± 0.09, n = 94 |
| | KO | | 1.79 ± 0.19, n = 105; p<0.04 |
| Fig. 2H (WB) | GluN2B | WT | 0.6832 ±0.04, n = 6 |
| | | KO | 0.9134 ± 0.08, n = 10; p<0.01 |
| Fig. 2H (qPCR) | GluN2B | WT | 1.00 ± 0.00, n = 8 |
| | | WT + Ro25 | 1.60 ± 0.19, n = 8; p<0.05 |
| | | KO | 1.26 ± 0.08, n = 8; p<0.05, compared to WT |
| Fig. 2I | WT | Ctrl | 73.1 ± 7.5 pA, n = 20 |
| | | Ro25 | 63.8 ± 7.6 pA, n = 17; p>0.1 |
| | | AP5 | 4.2 ± 0.6 pA, n = 9; p<0.001 |
| | KO | Ctrl | 99.2 ± 9.0 pA, n = 29; p<0.04, compared to WT-Ctrl |
| | | Ro25 | 74.3 ± 16.9 pA, n = 17; p>0.3 |
| | | AP5 | 5.1 ± 0.9 pA, n = 13; p<0.001 |
| Fig. 2L | WT | Ctrl | 29.2 ± 4.1 pC; n = 20 |
| | | Ro25 | 20.6 ± 5.3 pC; n = 17 |
| | KO | Ctrl | 34.3 ± 3.0 pC; n = 38 |
| | | Ro25 | 41.7 ± 6.2 pC; n = 29; p<0.04, compared to WT-Ro25 |
| Fig. 2N | Amplitude | WT | 107.4 ± 12.1 pA; n = 8 |
| | | KO | 38.5 ± 6.2 pA; n = 9; p<0.001 |
| | Charge | WT | 51.9 ± 10.1 pA; n = 8 |
| | | KO | 27.7 ± 4.6 pA; n = 9; p<0.05 |
| Fig. 2P (left) | WT | Ctrl | 40.8 ± 4.3 pC; n = 14 |
| | | Ro25 | 18.6 ± 3.3 pC; n = 14; p<0.001 |
| | KO | Ctrl | 45.7 ± 7.2 pC; n = 14 |
| | | Ro25 | 34.5 ± 5.5 pC; n = 14; p>0.4 |
| Fig. 2P (right) | WT | Ctrl | 18.9 ± 2.0 pC; n = 14 |
| | | Ro25 | 8.8 ± 1.5 pC; n = 14; p<0.001 |
| | KO | Ctrl | 21.5 ± 3.5 pC; n = 14 |
| | | Ro25 | 19.8 ± 5.0 pC; n = 14; p>0.1 |
| | | | |
| | | | Fig. 3 |

| | | | |
|---|---|---|---|
| Fig.3D | Scr | | $143.5 \pm 8.9$ s; n=15 |
| | Syt7 KD | | $103.6 \pm 6.9$ s; n=15; p<0.01 |
| | KD + Syt$^{IF4}$ | | $131.5 \pm 11.3$ s; n=15; p<0.01 |
| | KD + Syt$^{IF4mut}$ | | $96.5 \pm 9.6$ s; n=15; p>0.4 |
| Fig.3E | Scr | | $75.0 \pm 2.0$; n=15 |
| | Syt7 KD | | $82.7 \pm 2.6$; n=15; p<0.03 |
| | KD + Syt$^{IF4}$ | | $74.8 \pm 1.9$; n=15; p>0.9 |
| | KD + Syt$^{IF4mut}$ | | $87.8 \pm 5.1$; n=15; p<0.04 |
| Fig.3F | Scr | | $249.9 \pm 14.7$ s; n=15 |
| | Syt7 KD | | $348.1 \pm 7.6$ s; n=15; p<0.001 |
| | KD + Syt$^{IF4}$ | | $239.2 \pm 8.6$ s; n=15; p>0.5 |
| | KD + Syt$^{IF4mut}$ | | $361.0 \pm 6.8$ s; n=15; p<0.001 |
| Fig.3G | WT | Ctrl | $1.00 \pm 0.15$; n=3 |
| | | Ro25 | $2.07 \pm 0.08$; n = 3; p<0.03 |
| | KO | Ctrl | $1.44 \pm 0.16$, n = 3; p<0.05, compared to WT Ctrl |
| | | Ro25 | $0.99 \pm 0.12$, n = 3; p>0.08 |
| | KO + Syt$^{IF4}$ | Ctrl | $0.86 \pm 0.06$; n = 3; p>0.2, compared to WT Ctrl |
| | | Ro25 | $1.83 \pm 0.0921$; n = 3; p<0.02 |
| | KO + Syt$^{IF4mut}$ | Ctrl | $3.14 \pm 0.23$; n = 3; p<0.02, compared to WT Ctrl |
| | | Ro25 | $2.21 \pm 0.26$; n = 3; p>0.1 |
| Fig.3I | Scr | Ctrl | $1.05 \pm 0.19$ nC, n = 19 |
| | | Ro25 | $0.27 \pm 0.08$ nC, n = 22; p<0.001 |
| | KD | Ctrl | $1.43 \pm 0.16$ nC, n = 17 |
| | | Ro25 | $0.94 \pm 0.08$ nC, n = 14; p>0.07 |
| | KD + Syt$^{IF4}$ | Ctrl | $0.96 \pm 0.10$ nC, n = 27 |
| | | Ro25 | $0.39 \pm 0.08$ nC, n = 19; p<0.001 |
| | KD + Syt$^{IF4mut}$ | Ctrl | $1.55 \pm 0.12$ nC, n = 12 |
| | | Ro25 | $1.51 \pm 0.14$ nC, n = 16; p>0.8 |
| Fig.3J | Scr | Ctrl | $1.67 \pm 0.16$ s, n = 19 |
| | | Ro25 | $0.49 \pm 0.18$ s, n = 22; p<0.001 |
| | KD | Ctrl | $1.56 \pm 0.23$ s, n = 17 |
| | | Ro25 | $1.68 \pm 0.21$ s, n = 14; p>0.7 |
| | KD + Syt$^{IF4}$ | Ctrl | $1.81 \pm 0.11$ s, n = 27 |
| | | Ro25 | $1.27 \pm 0.21$ s, n = 19; p<0.001 |
| | KD + Syt$^{IF4mut}$ | Ctrl | $1.67 \pm 0.32$ s, n = 12 |
| | | Ro25 | $1.41 \pm 0.13$ s, n = 16; p>0.4 |
| Fig.3L | Scr | Ctrl | $17.22 \pm 2.44$ s, n = 10 |
| | | Ro25 | $8.22 \pm 0.74$ s, n = 10; p<0.001 |
| | | AP5 | $6.12 \pm 1.03$ s, n = 8; p<0.001, compared to Ctrl; p>0.1, compared to Ro25 |

| | | | |
|---|---|---|---|
| | KD | Ctrl | 15.62 ± 1.53 s, n = 8 |
| | | Ro25 | 18.06 ± 1.45 s, n = 8 |
| | | AP5 | 6.38 ± 0.58 s, n = 8; p<0.001, compared to Ctrl; p<0.001, compared to Ro25 |
| | KD + Syt$^{IF4}$ | Ctrl | 16.31 ± 1.60 s, n = 16 |
| | | Ro25 | 6.25 ± 0.68 s, n = 18; p<0.001 |
| | | AP5 | 7.51 ± 0.40 s, n = 16; p<0.001, compared to Ctrl; p>0.1, compared to Ro25 |
| | KD + Syt$^{IF4mut}$ | Ctrl | 20.01 ± 1.40 s, n = 21 |
| | | Ro25 | 17.30 ± 1.25 s, n = 20; p>0.1 |
| | | AP5 | 6.45 ± 0.65 s, n = 12; p<0.001, compared to Ctrl; p<0.001, compared to Ro25 |
| Fig.3M | Scr | Ctrl | 0.27 ± 0.05 pC, n = 10 |
| | | Ro25 | 0.10 ± 0.01 pC, n = 10; p<0.001 |
| | | AP5 | 0.06 ± 0.01 pC, n = 10; p<0.05 |
| | KD | Ctrl | 0.21 ± 0.03 pC, n = 8 |
| | | Ro25 | 0.22 ± 0.02 pC, n = 8; p>0.7 |
| | | AP5 | 0.08 ± 0.01 pC, n = 8; p<0.001, compared to Ctrl; p<0.001, compared to Ro25 |
| | KD + Syt$^{IF4}$ | Ctrl | 0.20 ± 0.04 pC, n = 16 |
| | | Ro25 | 0.08 ± 0.01 pC, n = 18; p<0.01 |
| | | AP5 | 0.08 ± 0.01 pC, n = 16; p<0.001, compared to Ctrl; p>0.2, compared to Ro25 |
| | KD + Syt$^{IF4mut}$ | Ctrl | 0.27 ± 0.04 pC, n = 21 |
| | | Ro25 | 0.25 ± 0.03 pC, n = 20; p>0.7 |
| | | AP5 | 0.08 ± 0.01 pC, n = 12; p<0.001, compared to Ctrl; p<0.001, compared to Ro25 |
| | | | |
| | | | Fig. 4 |
| Fig.4C | WT | 4 Ca$^{2+}$ | 0.14 ± 0.02 at 2.5 s; 0.27 ± 0.04 at 5 s; 0.31 ± 0.04 at 7.5 s; 0.31 ± 0.05 at 10 s; n = 104 |
| | | 0.2 Ca$^{2+}$ | 0.05 ± 0.01 at 2.5 s; 0.14 ± 0.02 at 5 s; 0.21 ± 0.03 at 7.5 s; 0.25 ± 0.03 at 10 s; n = 99 |
| | | 0.2 Sr$^{2+}$ | 0.11 ± 0.01 at 2.5 s; 0.30 ± 0.03 at 5 s; 0.39 ± 0.04 at 7.5 s; 0.38 ± 0.04 at 10 s; n = 98 |
| | Syt7 KO | 4 Ca$^{2+}$ | 0.08 ± 0.01 at 2.5 s; 0.22 ± 0.04 at 5 s; 0.31 ± 0.05 at 7.5 s; 0.32 ± 0.05 at 10 s; n = 96 |

| | | | |
|---|---|---|---|
| | | 0.2 Ca$^{2+}$ | 0.02 ± 0.01 at 2.5 s;<br>0.07 ± 0.01 at 5 s;<br>0.12 ± 0.02 at 7.5 s;<br>0.17 ± 0.02 at 10 s; n = 101 |
| | | 0.2 Sr$^{2+}$ | 0.03 ± 0.01 at 2.5 s;<br>0.08 ± 0.02 at 5 s;<br>0.10 ± 0.03 at 7.5 s;<br>0.10 ± 0.04 at 10 s; n = 94 |
| | KO + Syt7$^{FL}$ | 4 Ca$^{2+}$ | 0.08 ± 0.01 at 2.5 s;<br>0.19 ± 0.02 at 5 s;<br>0.28 ± 0.03 at 7.5 s;<br>0.32 ± 0.03 at 10 s; n = 95 |
| | | 0.2 Ca$^{2+}$ | 0.02 ± 0.01 at 2.5 s;<br>0.06 ± 0.02 at 5 s;<br>0.10 ± 0.02 at 7.5 s;<br>0.17 ± 0.03 at 10 s; n = 76 |
| | | 0.2 Sr$^{2+}$ | 0.05 ± 0.01 at 2.5 s;<br>0.14 ± 0.02 at 5 s;<br>0.23 ± 0.03 at 7.5 s;<br>0.27 ± 0.04 at 10 s; n = 78 |
| | KO + Syt7$^{IF4mut}$ | 4 Ca$^{2+}$ | 0.06 ± 0.01 at 2.5 s;<br>0.15 ± 0.02 at 5 s;<br>0.21 ± 0.03 at 7.5 s;<br>0.24 ± 0.03 at 10 s; n = 79 |
| | | 0.2 Ca$^{2+}$ | 0.02 ± 0.00 at 2.5 s;<br>0.06 ± 0.01 at 5 s;<br>0.09 ± 0.02 at 7.5 s;<br>0.13 ± 0.03 at 10 s; n = 88 |
| | | 0.2 Sr$^{2+}$ | 0.02 ± 0.00 at 2.5 s;<br>0.04 ± 0.01 at 5 s;<br>0.06 ± 0.03 at 7.5 s;<br>0.09 ± 0.02 at 10 s; n = 64 |
| Fig.4D | WT | 4 Ca$^{2+}$ | 0.31 ± 0.04; n = 104 |
| | | 0.2 Ca$^{2+}$ | 0.25 ± 0.03; n = 99 |
| | | 0.2 Sr$^{2+}$ | 0.38 ± 0.04; n = 98; p<0.005, compared to 0.2Ca$^{2+}$ |
| | Syt7 KO | 4 Ca$^{2+}$ | 0.32 ± 0.05; n = 96 |
| | | 0.2 Ca$^{2+}$ | 0.17 ± 0.02; n = 101; p<0.01, compared to 4Ca$^{2+}$ |
| | | 0.2 Sr$^{2+}$ | 0.10 ± 0.03; n = 94; p<0.003, compared to 4Ca$^{2+}$;<br>p<0.05, compared to 0.2Ca$^{2+}$ |
| | KO + Syt7$^{FL}$ | 4 Ca$^{2+}$ | 0.31 ± 0.03; n = 95 |
| | | 0.2 Ca$^{2+}$ | 0.17 ± 0.03; n = 76; p<0.01, compared to 4Ca$^{2+}$ |
| | | 0.2 Sr$^{2+}$ | 0.27 ± 0.03; n = 78; p<0.02, compared to 0.2Ca$^{2+}$ |
| | KO + Syt7$^{IF4mut}$ | 4 Ca$^{2+}$ | 0.24 ± 0.03 at 10 s; n = 79 |
| | | 0.2 Ca$^{2+}$ | 0.13 ± 0.03 at 10 s; n = 88; p<0.01, compared to 4Ca$^{2+}$ |
| | | 0.2 Sr$^{2+}$ | 0.09 ± 0.02 at 10 s; n = 64; p<0.001, compared to 4Ca$^{2+}$ |
| Fig.4F | WT | 4 Ca$^{2+}$ | 1.13 ± 0.04; n = 104 |

| | | | |
|---|---|---|---|
| | | 0.2 Ca$^{2+}$ | 1.18 ± 0.04; n = 99 |
| | | 0.2 Sr$^{2+}$ | 1.20 ± 0.05; n = 98 |
| | Syt7 KO | 4 Ca$^{2+}$ | 1.03 ± 0.03; n = 96, p<0.05, vs. WT |
| | | 0.2 Ca$^{2+}$ | 1.03 ± 0.04; n = 101, p<0.01, vs. WT |
| | | 0.2 Sr$^{2+}$ | 1.06 ± 0.04; n = 94, p<0.03, vs. WT |
| | KO + Syt7$^{FL}$ | 4 Ca$^{2+}$ | 1.08 ± 0.05; n = 95, p>0.1, vs. KO |
| | | 0.2 Ca$^{2+}$ | 1.26 ± 0.06; n = 76, p<0.01, vs. KO |
| | | 0.2 Sr$^{2+}$ | 1.17 ± 0.04; n = 78, p<0.05, vs. KO |
| | KO + Syt7$^{IF4mut}$ | 4 Ca$^{2+}$ | 1.05 ± 0.04; n = 79, p>0.1, vs. KO |
| | | 0.2 Ca$^{2+}$ | 0.92 ± 0.08; n = 88, p<0.01, vs. KO |
| | | 0.2 Sr$^{2+}$ | 0.99 ± 0.04; n = 64, p<0.05, vs. KO |
| | | | |
| Fig. 5 | | | |
| Fig.5D | WT | 0.66 ± 0.06 nA, n = 18 | |
| | Syt7 KO | 0.59 ± 0.04 nA, n = 18; p>0.4, compared to WT | |
| | KO + Syt7$^{FL}$ | 0.59 ± 0.09 nA, n = 15; p>0.5, compared to WT | |
| | KO+Syt7$^{GAP43}$ | 0.30 ± 0.01 nA, n = 21; p<0.001, compared to WT | |
| Fig.5H (total charge) | WT | Ctrl | 447.4 ± 62.8 pC, n = 14 |
| | | Ro25 | 160.6 ± 25.0 pC, n = 14; p<0.001 |
| | KO | Ctrl | 433.3 ± 70.4 pC, n = 14 |
| | | Ro25 | 373.9 ± 81.3 pC, n = 14; p>0.1 |
| | KO + Syt7$^{FL}$ | Ctrl | 377.6 ± 75.2 pC, n = 14 |
| | | Ro25 | 156.9 ± 38.3 pC, n = 14; p<0.001 |
| | KO + Syt7$^{GAP43}$ | Ctrl | 309.0 ± 24.7 pC, n = 14 |
| | | Ro25 | 272.9 ± 25.9 pC, n = 14; p>0.3 |
| Fig.5H (decay tau) | WT | Ctrl | 1.8 ± 0.2 s, n = 14 |
| | | Ro25 | 1.3 ± 0.1 s, n = 14; p<0.05 |
| | KO | Ctrl | 2.1 ± 0.4 s, n = 14 |
| | | Ro25 | 1.9 ± 0.2 s, n = 14; p>0.2 |
| | KO + Syt7$^{FL}$ | Ctrl | 1.7 ± 0.2 s, n = 14 |
| | | Ro25 | 1.1 ± 0.1 s, n = 14; p<0.05 |
| | KO + Syt7$^{GAP43}$ | Ctrl | 2.0 ± 0.2 s, n = 14 |
| | | Ro25 | 1.8 ± 0.2 s, n = 14; p>0.3 |
| | | | |
| Fig. 6 | | | |
| Fig.6B | HC | 118.7 ± 6.7; n = 4 lines | |
| | BD-I | 68.8 ± 5.4; n = 6 lines | |
| Fig.6C | HC | 1.16 ± 0.06; n = 4 lines | |
| | BD-I | 1.75 ± 0.09; n = 6 lines | |
| Fig.6D | GluN2A | HC | 0.18 ± 0.01; n = 4 lines |

| | | | | |
|---|---|---|---|---|
| | | | BD-I | 0.24 ± 0.01; n = 6 lines; p<0.01 |
| | GluN2B | | HC | 0.16 ± 0.02; n = 4 lines |
| | | | BD-I | 0.27 ± 0.03; n = 6 lines; p<0.01 |
| Fig.6G | HC | | | 170.42 ± 10.58 pC; n = 4 lines |
| | BD | | | 197.31 ± 7.35 pC; n = 6 lines; p>0.1 |
| Fig.6H | HC | #1 | Ctrl | 146.23 ± 26.86 pC; n = 20 |
| | | | Ro25 | 67.01 ± 9.22 pC; n = 13; p<0.02 |
| | | #2 | Ctrl | 162.69 ± 16.89 pC; n = 21 |
| | | | Ro25 | 64.58 ± 7.92 pC; n = 23; p<0.001 |
| | | #3 | Ctrl | 176.65 ± 20.63 pC; n = 31 |
| | | | Ro25 | 74.61 ± 6.48 pC; n = 51; p<0.001 |
| | | #4 | Ctrl | 196.11 ± 14.35 pC; n = 44 |
| | | | Ro25 | 100.72 ± 7.82 pC; n = 25; p<0.001 |
| | BD-I | #1 | Ctrl | 186.05 ± 19.61 pC; n = 17 |
| | | | Ro25 | 152.49 ± 15.79 pC; n = 17 |
| | | #2 | Ctrl | 190.85 ± 19.44 pC; n = 25 |
| | | | Ro25 | 155.01 ± 17.47 pC; n = 25 |
| | | #3 | Ctrl | 203.26 ± 16.42 pC; n = 30 |
| | | | Ro25 | 226.74 ± 16.04 pC; n = 32 |
| | | #4 | Ctrl | 212.90 ± 14.22 pC; n = 35 |
| | | | Ro25 | 230.17 ± 14.66 pC; n = 43 |
| | | #5 | Ctrl | 171.28 ± 23.82 pC; n = 41 |
| | | | Ro25 | 130.89 ± 12.14 pC; n = 31 |
| | | #6 | Ctrl | 219.53 ± 20.33 pC; n = 20 |
| | | | Ro25 | 199.43 ± 20.53 pC; n = 23 |
| | BD-I + Syt7 | #1 | Ctrl | 158.21 ± 28.86 pC; n = 13 |
| | | | Ro25 | 88.57 ± 25.50 pC; n = 13; p<0.001 |
| | | #5 | Ctrl | 206.44 ± 38.97 pC; n = 13 |
| | | | Ro25 | 119.29 ± 25.87 pC; n = 11; p<0.04 |
| | | #6 | Ctrl | 117.34 ± 18.82 pC; n = 17 |
| | | | Ro25 | 66.20 ± 10.88 pC; n = 26; p<0.02 |
| | | | | |
| | | | Fig. S1 | |
| Fig.S1A (WB) | GluN2A | WT | | 0.56 ± 0.06, n = 6; |
| | | KO | | 0.78 ± 0.04, n = 10; p<0.05 |
| Fig.S1A (qPCR) | GluN2A | WT | | 1.00 ± 0.00, n = 8; |
| | | WT + Ro25 | | 2.49 ± 0.26, n = 8; p<0.01, compared to WT |
| | | KO | | 1.60 ± 0.11, n =8; p<0.01, compared to WT |
| | GluN1 | WT | | 1.00 ± 0.00, n = 8 |
| | | WT + Ro25 | | 1.41 ± 0.11, n = 8; p<0.01, compared to WT |
| | | KO | | 1.36 ± 0.06, n = 8; p<0.01, compared to WT |